Analysis of a Microwave Time Delay Line Based on a Perturbed Uniform Fiber Bragg Grating Operating at Constant Wavelength

Beatriz Ortega, José L. Cruz, José Capmany, Miguel V. Andrés, and Daniel Pastor

***Abstract*—This paper presents the modeling of a new microwave time delay line based on a uniform fiber Bragg grating (FBG) with a section which period has been perturbed. The time delay can be modified by changing the position of the perturbation along the grating. Theoretical results are presented for a 5-cm long uniform grating and optical signal is modulated up to 18 GHz. Experimental setup used magnetic fields to change the period locally along the grating and a 330 ps maximum time delay is shown. Comparison between calculations and measurements show a perfect agreement. Such a delay line offers many advantages for beamforming applications in phased array antennas where the operation at a fixed wavelength is required in order to simplify the architecture of these systems.**

***Index Terms*—Bragg gratings, delay lines, fiber optics, microwave photonics.**

I. Introduction

DURING the last decade there has been an intense research in optical beamforming networks for phased array antennas [1]–[3]. Recent developments of optical fiber gratings have increased the possibilities of implementing time delay lines for driving microwave antennas. In these systems, an optical fiber is used to guide the optical carrier of an radio frequency (RF) modulating signal that drives every element of the array. The use of optical fibers to distribute the signal has many advantages such as low insertion loss, high phase stability, electromagnetic inmunity and the possibility of controlling several arrays by using wavelength-division-multiplexing (WDM) techniques, apart from the low mass and costs that also characterize optical fiber systems.

In the first approaches, beamforming networks are based on uniform fiber gratings written at different positions on optical fibers [4]–[6], and the distances between gratings determine the beampointing direction. A WDM system or a timing unit can be used to distribute the optical carrier to the radiators. This system assures broadband operation but it only allows a discrete number of beampointing angles [7].

However, chirped fiber Bragg gratings have been recently demonstrated as linear phase-shifters at microwave frequencies [8], and the slope of the phase response versus frequency can be modified by changing the wavelength of the optical carrier. The amplitudes and phases of the RF-modulating reflected signal are used to drive the radiating elements by means of a WDM scheme and the time delay difference between adjacent carriers determines the beampointing angle of the antenna. Broadband operation and continuous spatial scanning properties have been demonstrated in these systems, although the variety of optical carriers requires a complex demultiplexing stage, which is desirable to be simplified in practical systems [9]–[11].

In this paper, we propose and analyze a novel variable time delay line operating at a fixed wavelength, which simplifies the architecture of the beamforming system exposed above. It is based on an uniform fiber Bragg grating with a section which period has been modified by an external actuator. The optical carrier is reflected by the perturbed section of the grating and the time delay is modified by changing the position of the perturbation along the grating. In Section II we describe the operation of the time delay line, Section III gives the theoretical response of this system and Section IV shows the comparison of the experimental results with the theoretical ones. Finally, Section V will summarize the obtained results and conclude the paper.

II. Device Operation

We consider an uniform fiber grating with the Bragg wavelength λ_B, and a local section within it whose period is perturbed, and therefore, its resonant wavelength is $\lambda_C \neq \lambda_B$ (see Fig. 1). An optical carrier of wavelength λ_C is reflected by the perturbed section and will travel along different fiber lengths given by L_{eff}, depending on the position of this section, X. Therefore, if the carrier is modulated by a microwave signal of frequency $\Omega = 2\pi f_{\text{RF}}$, the modulating signal suffers a phase delay given by

$$\Delta\Phi_{\text{RF}} = \Omega\tau(X) \tag{1}$$

where $\tau(X)$ is the transit time along the grating and is given by the fiber length traversed by the light "$2L_{\text{eff}}(X)$"

$$\tau(X) = \frac{2L_{\text{eff}}(X)n}{c} \tag{2}$$

where n_{eff} is the effective refractive index along the grating and c is the velocity of light.

Hence, the grating produces a linear phase shift in the modulating signal and the phase slope can be continuously varied by displacing the perturbed section along the grating [12], [13]. Note that the device behaves as a true-time delay line provided

Manuscript received July 2, 1999; revised November 24, 1999. This work was supported by the DGCYT of Spain under Grants TIC98-0346 and TIC97-1153).

J. Capmany, and D. Pastor are with the Departamento de Comunicaciones, Universidad Politécnica de Valencia, Valencia 46022, Spain.

J. L. Cruz and M. V. Andrés are with the Departamento de Física Aplicada, Universidad de Valencia, Burjassot 46100, Spain.

Publisher Item Identifier S 0733-8724(00)02199-X.

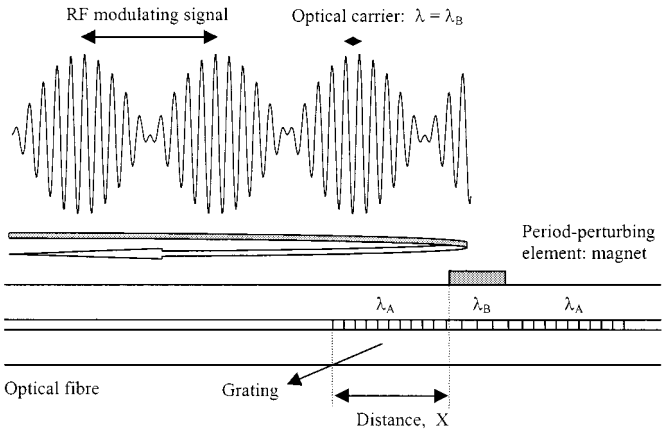

Fig. 1. Schematic of the phase shifter setup based on a uniform FBG with a perturbed section.

that the time delay of the modulated signal is independent of the modulating frequency, i.e., the modulation frequency is lower enough to preserve the linewidth of the optical light spectrum.

The grating is formed by three uniform sections with Bragg wavelengths λ_1, λ_2 and λ_3, the transmission matrix of the grating T can be calculated from the transmission matrix of each section T_i:

$$T = T_1(L_1, \lambda_A) \cdot T_2(L_2, \lambda_B) \cdot T_3(L_3, \lambda_A) \tag{3}$$

and the reflection cofficient of the grating "r" can be obtained from the elements of the transmission matrix [14]:

$$\rho = \frac{-T_{21}}{T_{22}}. \tag{4}$$

If the optical carrier of frequency ω modulated by a signal of RF frequency Ω by using a double sideband technique, for low-modulation rates, the spectrum of the modulated signal has three frequency components: the carrier $e^{j\omega t}$ and two sidebands $e^{j(\omega+\Omega)t}$ and $e^{j(\omega-\Omega)t}$. If the optical signal is reflected by the fiber grating with a reflection coefficient of $\rho(\omega) = |\rho(\omega)|e^{j\theta(\omega)}$, then the reflected electric field in the fiber is a sum of the following terms:

$$\rho(\omega)e^{j\omega t}; \rho(\omega-\Omega)e^{j(\omega-\Omega)t}; \rho(\omega+\Omega)e^{j(\omega+\Omega)t}. \tag{5}$$

After the detection by using a fast photodiode, the electric field in the microwave transmission line is a sum of harmonics of the modulating frequency Ω high-order harmonics can be neglected for weak modulations and the RF field can be expressed as

$$E(t) = E(\Omega, \omega)e^{j(\Omega t + \Psi(\Omega,\omega))} \tag{6}$$

where amplitudes $E(\Omega, \omega)$ and phases $\phi(\Omega, \omega;)$are the following [8]:

$$\begin{aligned} E(\Omega,\omega) = \frac{1}{2}|\rho(\omega)| \cdot [&(|\rho(\omega+\Omega)|\cos(\theta(\omega+\Omega)-\theta(\omega)) \\ &+|\rho(\omega-\Omega)|\cos(\theta(\omega)-\theta(\omega-\Omega)))^2 \\ &+(|\rho(\omega+\Omega)|\sin(\theta(\omega+\Omega)-\theta(\omega)) \\ &+|\rho(\omega-\Omega)|\sin(\theta(\omega)-\theta(\omega-\Omega)))^2]^{1/2} \end{aligned}$$

$$\Psi(\Omega,\omega) = \text{arctg}\left[\frac{\begin{array}{c}(|\rho(\omega+\Omega)|\sin(\theta(\omega+\Omega)-\theta(\omega)) \\ +|\rho(\omega-\Omega)|\sin(\theta(\omega)-\theta(\omega-\Omega)))\end{array}}{\begin{array}{c}(|\rho(\omega+\Omega)|\cos(\theta(\omega+\Omega)-\theta(\omega)) \\ +|\rho(\omega-\Omega)|\cos(\theta(\omega)-\theta(\omega-\Omega)))\end{array}}\right]. \tag{7}$$

Provided the modulating frequency is smaller than the grating bandwidth, (7) can be approximated by the following:

$$\begin{aligned} E(\Omega,\omega) &= |\rho(\omega)|^2 \\ \Psi(\Omega,\omega) &= \frac{\theta(\omega+\Omega)-\theta(\omega-\Omega)}{2}. \end{aligned} \tag{8}$$

Therefore, the phase of the RF signal satisfies (1) where $\tau(\omega) = (d\theta(\omega)/d\omega)$ is the time delay response of the fiber grating.

Hence, provided the modulating frequency is low enough to maintain the bandwidth of the optical carrier, the phase of the RF signal presents a linear behavior with the modulating frequency Ω, and the slope can be varied by changing the time delay of the optical carrier, which is given by the position of the perturbed section.

The operation of this system is based on fixing the optical wavelength at the sideband. The amplitude and phase of the signal are used to steer every element in a phased array antenna, provided the bandwidth of the modulated signal is smaller than the bandwidth of the altered side-band of the grating.

A beamforming system for phased array antennas based on this time delay line operates at a fixed optical wavelength does not need any demultiplexing stage and, therefore, is simpler and cheaper than other multiwavelength approaches. Such a system requires one delay line for driving every element of the antenna (see Fig. 2). The optical signal at λ_C is modulated and distributed to all of them. The positions of the perturbed sections in every line will be addressed by an automatic system in order to provide the distribution of amplitudes and phases which are convinient to achieve the desired radiation pattern of the antenna.

III. Theoretical Results

In the modeling of the device, we used a 5-cm-long strong uniform grating ($KL = 15\pi$) with its bandpass centered at $\lambda_B = 1526.1$ nm and a 3-dB bandwidth of 0.7 nm. The reflectivity of the grating is shown in Fig. 3(a). By increasing the Bragg wavelength of a 2.5-mm section ($X = 25$ mm) of the grating by a 0.06%, the grating reflectivity shows a strong sidelobe centered at $\lambda_C = 1527.0$ nm, as it is shown in Fig. 3(b) with similar bandwidth as the original bandpass due to the large intensity of the coupling provoqued by the grating.

By locating the perturbed section at different positions along the grating, we find, as expected, the reflectivity response does not change significantly—see Fig. 4(a). However, looking at the time delay response of the grating, the time characteristic of the emerging sideband is dependent on the position of the perturbed section since the local reflection of this wavelength is happening at different positions along the fiber which means different travelling-time of the signal. Fig. 4(b) shows the time delay response of the original grating when a 2.5-mm period-increased section is placed at $X = 5$ mm from the initial end (solid line) and when

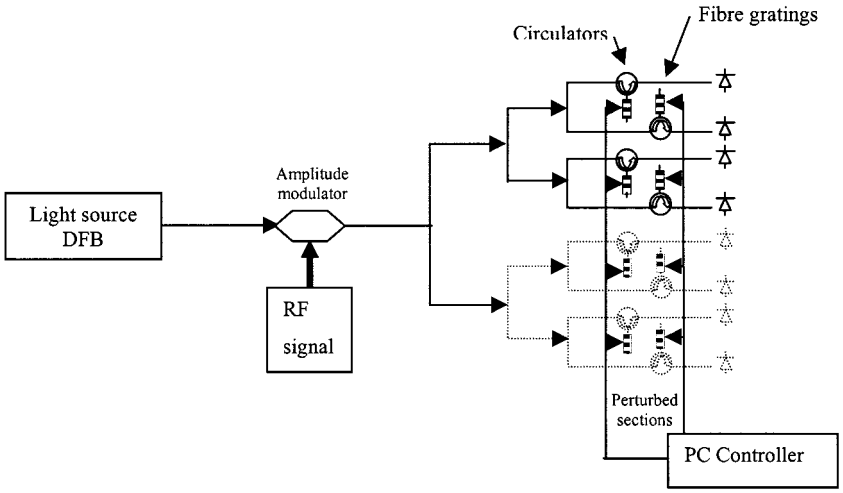

Fig. 2. Schematic of the beamforming system for microwave phased array antennas based on uniform FBG's.

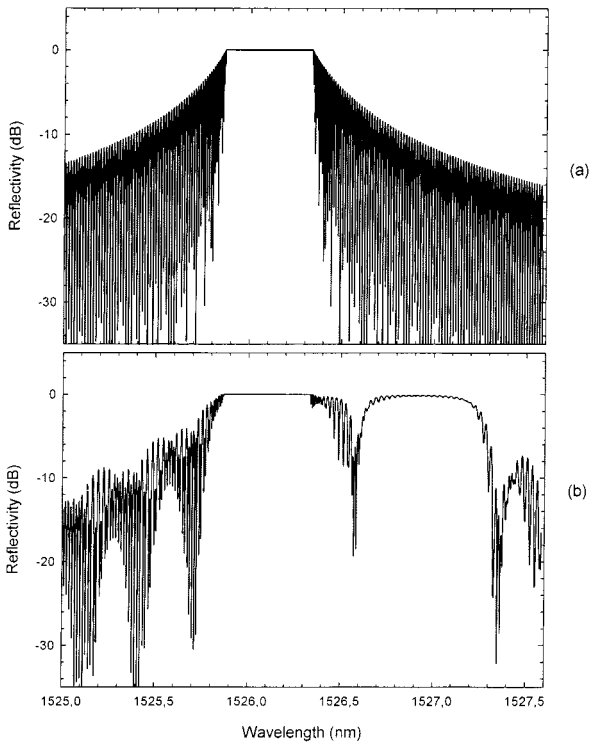

Fig. 3. Spectral reflectivity of the original uniform grating (a) and the same when the period of a section of the grating is perturbed (b).

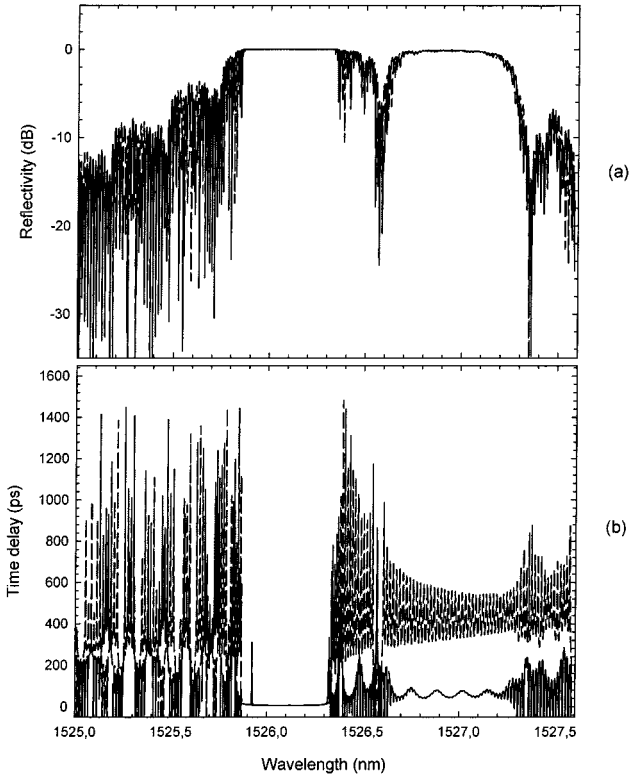

Fig. 4. Spectral reflectivity (a) and time delay response (b) of the grating, with the perturbed area (2.5 mm) at two different positions: (solid line) $X = 5$ mm, (dashed line) $X = 40$ mm.

the same perturbation is placed at $X = 40$ mm. The average time delay values difference is $\Delta\tau = 372$ ps, which corresponds to a return trip of the signal along a distance of 37 mm in a material with a refraction index $n = 1.5$, according to the spacing of 35 mm, which was set for the calculations. Note the rippled characteristic along the sideband, which period decreases and amplitude increases as long as we increase the distance X of the perturbed section respect to the initial end of the grating. The oscillations are due to the formation of a Fabry–Perot cavity between the uniform sub-gratings existing inside the original grating. In this case, due to the intense grating, the cavity is formed by the initial ends of the original grating and the perturbed section. The period of the oscillations decreases with the distance X ($\Delta\nu = c/2X$), and their amplitude increases with X. The periodicities at $X = 5$ and 40 mm are $\Delta\lambda = 0.137$ and 0.0198 nm, respectively, corresponding to cavity lengths of 5.8 and 40.4 mm, as expected from the values we employed in the simulation.

The behavior of the delay line was analyzed by means of equation [7] by setting the optical wavelength at $\lambda = 1527$ nm and modulating with a microwave signal. Fig. 5 shows the amplitude response at different modulating frequencies in the range [130 MHz—18 GHz] when the perturbed section is at position given by $X = 5$ and $X = 45$. The curve corresponding to

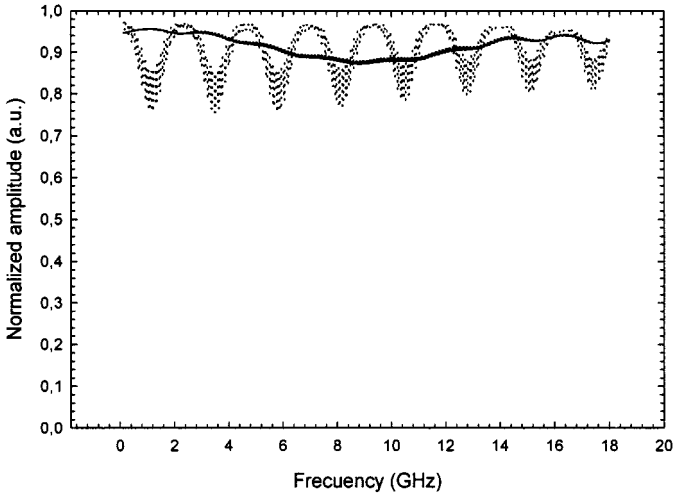

Fig. 5. Signal amplitude at different modulating frequencies for two different positions of the perturbed section (————) 5 mm y (· · · · · · · · ·) 45 mm.

the last one shows the oscillation arising from the Fabry–Perot cavity with a periodicity of 2.28 GHz, corresponding to a 44-mm long cavity, according to the distance between initial ends of original and perturbed gratings. Table I shows the mean values of the normalized amplitude and their standard deviations at different positions along the grating.

The calculated phase of the signal for the same frequency range is shown in Fig. 6 when perturbed section is located at different positions, spaced by 5 mm, along the grating, all measured from the initial end of the original grating. Note the slight oscillation due to the Fabry–Perot cavity, which amplitude increases with the cavity length. At $X = 25$ mm, the root-mean-square (rms). deviation value from a linear fit is about 0.17 rad. The ripple of these curves determines the aberrations of the phase distribution in radiating elements of an antenna; the phase deviation value leads to a time delay fluctuation under 2 ps at maximum operating frequency of 18 GHz, which is acceptable for good array performance.

The phase shows a linear characteristic with a slope which can be varied by perturbing the original grating at a different position. Table II shows the phase slope values (rad/GHz) and their corresponding time delay values. Fig. 7 shows the linear behavior of the time delay values versus the position X of the perturbed section with the corresponding fit, which slope gives information about the propagation velocity of the optical signal travelling through the grating in the optical fiber. The slope is of 10.78, which means a velocity of $1.85 \cdot 10^8$ m/s in a return trip along the grating.

However, this system has a large degree of freedom related to the wavelength of the optical carrier. By varying the period in different amounts, the emerging sideband, i.e. the optical carrier, is located at different wavelengths in the spectrum. Fig. 8 shows the spectral reflectivity of the grating when a 2.5-mm section has a 0.06% modified Bragg wavelength [see Fig. 3(b)] and when the perturbation is about 0.10%, which shows the sideband centered at $\lambda_D = 1527.9$ nm. This wavelength can be continuously tuned by varying the intensity of the perturbation. Furthermore, if two sections of the grating are perturbed

TABLE I
MEAN VALUES AND STANDARD DEVIATIONS OF THE AMPLITUDE OF THE MODULATING SIGNAL WHEN THE PERTURBED SECTION IS LOCATED AT DIFFERENT POSITIONS ALONG THE GRATING

X (mm)	$\overline{R}$ (dBm)	$\varepsilon_{\overline{R}}$ (dB)
0	-0,18	0,02
5	-0,36	0,14
10	-0,13	0,05
15	-0,36	0,14
20	-0,46	0,25
25	-0,22	0,14
30	-0,27	0,05
35	-0,36	0,24
40	-0,41	0,30
45	-0,32	0,09

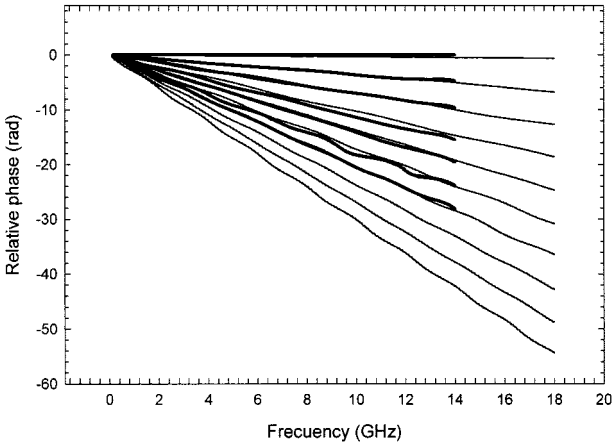

Fig. 6. Phase of the modulated signal at different RF frequencies after reflection by the perturbed section of the grating when this is located at different positions along the original grating (solid line). Experimental data (Δ).

TABLE II
PHASE/FREQUENCY SLOPE AND THE CORRESPONDING TIME DELAY VALUE FOR DIFFERENT POSITIONS OF THE PERTURBED SECTION ALONG THE GRATING. COMPARISON BETWEEN CALCULATED AND MEASURED RESULTS

Position	Phase/Frecuency (rad/GHz)		Time delay τ (ps)	
X (mm)	Theoretical	Experimental	Theoretical	Experimental
0	-0.03	0	4,77	0
5	-0.37	-0.36	58,89	57,30
10	-0.71	-0.70	113,00	111,41
15	-1.03	-1.13	163,93	179,84
20	-1.37	-1.40	218,04	222,82
25	-1.70	-1.76	270,56	280,11
30	-2.03	-2.03	323,08	323,08
35	-2.37		377,20	
40	-2.70		429,72	
45	-3.03		482,24	

by different amounts, two optical carriers can be employed simultaneously. Fig. 9 shows the reflectivity response of a grating

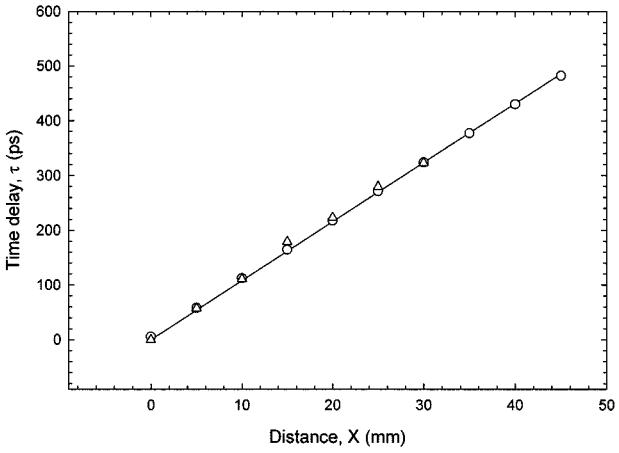

Fig. 7. Time delay values corresponding to different positions of the perturbed section of the grating (O,theoretical data and fit). Positions are measured respect to the initial end of the original grating. Experimental data (Δ).

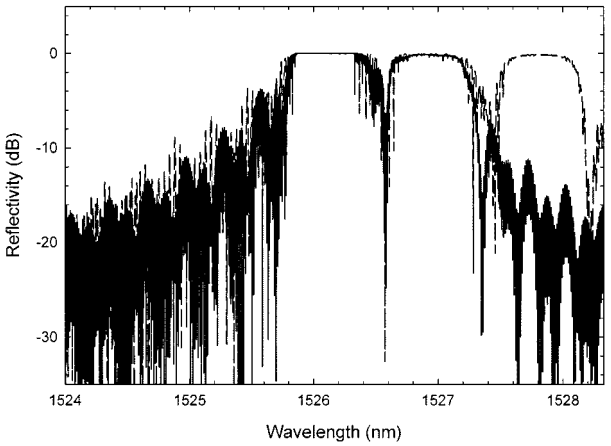

Fig. 8. Reflectivity response of the grating with two differently perturbed sections: Use of two optical carriers.

with two 2.5-mm-long sections perturbed by 0.06% and 0.12%, where the bandwidth of the sidebands impose a limitation on the proximity of the two optical carriers. The spacing between sections gives the time delay difference corresponding to the modulating signal of both optical carriers, which can also be used for multiple phased arrays steering applications.

IV. Experimental Results

Experimental setup is based on a 5-cm-long uniform grating, which is held on a magnetostrictive rod ($Tb_{0.27}Dy_{0.73}Fe_2$) with a sensitivity of 10 ppm/mT [15], and a small part of the grating is strained by the effect of a magnetic field created by a 10-mm-long cylindrical magnet with a diameter of 22 mm (maximum magnetic field of 120 mT). Hysteresis of the magnetostrictive material is under 7%, which does not affect to the performance of our system; and the response time is in the [0.04–0.2] ms range, which is also typical for piezoelectric transducer (PZT) materials suitable for this application. The light source is a tunable laser and the amplitude of the signal was externally modulated by an RF signal. The reflected light is driven by a 3-dB coupler to the detection in an optical network analyzer [16]. The reflectivity response of the grating is shown in Fig. 10 (solid line) and shows the bandpass centered at 1526.1 nm and its 3 dB-bandwidth of 0.7 nm. Dashed line shows the resulting spectra when the magnetic field is applied, i.e., the magnet is placed at a distance $X = 40$ mm from the initial end of the original grating. The grating spectrum preserves the flat response of the original grating at 1526.1 nm and a secondary peak appears at 1527.0 nm with 0.3 nm bandwidth, corresponding to the Bragg wavelength of the part of the grating strained by the magnet. In alternative setups, this effect in the response of the grating can be created by voltages of 100 V applied to a PZT or about 1-A current in a magnetic coil.

The time delay response of the grating when the magnet is located at different positions along the grating is shown in Fig. 11. The graph shows a good agreement with the theoretical calculations (Fig. 7) and we observe a different average time value for each position in the secondary peak, while the response in other

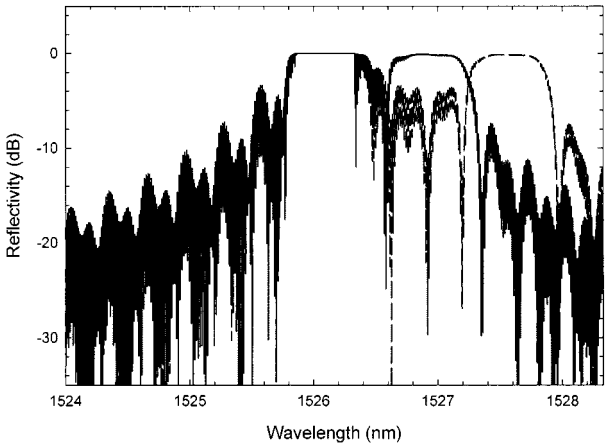

Fig. 9. Tunable optical carrier. Reflectivity response when the period of the grating is perturbed by different amounts: (a) 0.06% and (b) 0.12%.

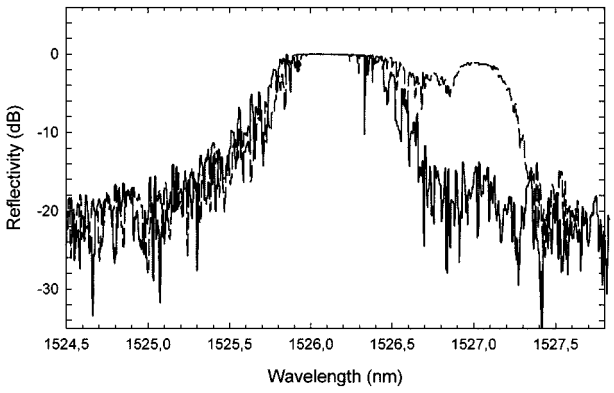

Fig. 10. Measured reflectivity of the grating: (a) Original grating. (b) Grating when the period of a section is perturbed at $X = 40$ mm.

parts of the spectrum remains the same. This effect is due to the fact that the signal which is travelling different length along the grating is, basically, the one reflected by the perturbed section. Note that rippled characteristic in the secondary peak which was observed in Fig. 7 is also seen in the experimental measurements. Although this magnet can be placed in arbitrary positions along the grating, in practical systems the actuators must

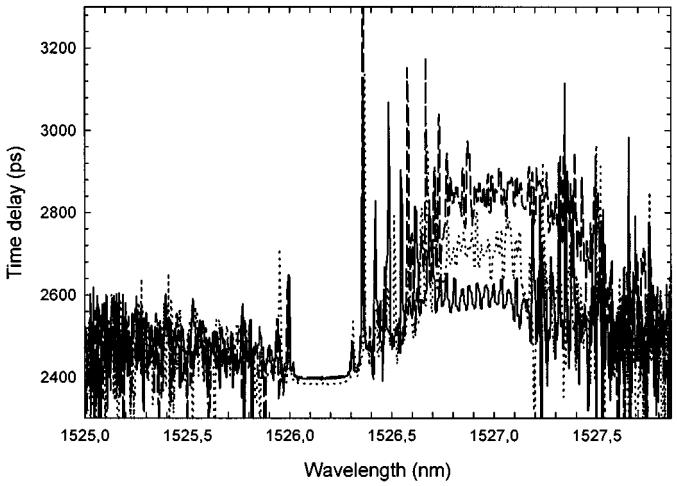

Fig. 11. Time delay response of the grating when perturbed section is located at three different positions: (————) 20 mm, (· · · · · · · · ·) 32 mm, (– – – – –) 44 mm.

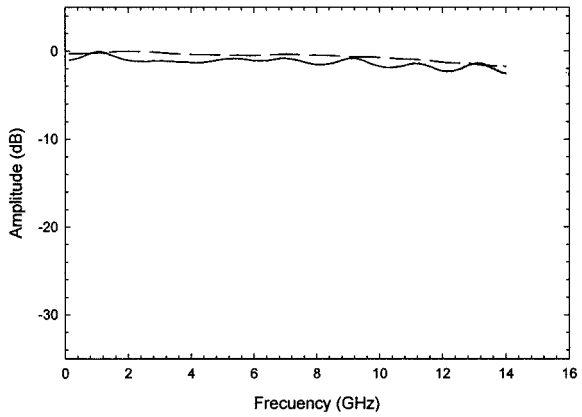

Fig. 12. Amplitude of the signal when optical wavelength is fixed and the perturbed section is located at two different positions: (– – – – –) 15 mm and (————) 45 mm.

be fixed to the grating, we estimate that the minimum distance between adjacent perturbations could be (1 mm so the smallest time delay variation will be about 10 ps.

To test the grating as a microwave shifter the laser output was set at the wavelength of 1527 nm and the linewidth of the modulated light (about 0.22 nm at 14 GHz) was smaller than the bandwidth of the grating sidelobe (0.30 nm). Fig. 6 shows the phase of the microwave signal after reflection in the grating (triangles), presenting a linear dependence on the frequency in the 1–14 GHz range, and showing a good agreeement with the calculated results. According to previous section, the phase slope can be controlled by changing the position of the magnet along the grating. The r.m.s. deviation value from the ideal linear behavior is 0.30 rad in the worst case (curve at $X = 25$ mm), slightly higher than theoretical prediction.

The delay corresponding to each curve can be calculated from the slope following (1), and the obtained results are plotted in Fig. 7 (triangles) together with the theoretical values. Note the linear dependence on the magnet position and the good agreement between measurements and calculations. The measurements indicate that the strained part of the grating has a well defined phase centre, probably because of the strength of the grating. We estimate a delay error from linearity about 4, 1.4, 2.4, 11.6, 1.1, 3, 8.2 ps at different positions from $x = 0$ to $x = 30$ mm. These deviations are mainly due to our experimental setup, where the uncertainty in the position of the perturbed section is about 1 mm, which means a time delay deviation of 10 ps, although these values can be easily improved by a factor of 10 in other setups.

Also, the amplitude of the signal at different RF frequencies was measured for different positions of the magnet, and results very similar to those exposed in the previous section were obtained. Fig. 12 shows the amplitude when the optical wavelength is 1527 nm and the perturbed section is located at 15 and 45 mm from the initial end. A slight oscillation of the signal with frequency appears due to the Fabry–Perot cavity formed by the two embedded gratings, and periodicity decreases with the distance to the initial end.

V. Conclusion

We have analyzed and experimentally demonstrated a novel time delay line based on a uniform FBG for microwave applications. The device operates at a single optical wavelength and the time delay is tuned by increasing the period of a region of the grating. Experimental setup used magnetic fields to apply a local strain at different positions along the grating and the obtained measurements showed a very good agreement with the theoretical calculations. By using a 5-cm-long grating operation was demonstrated up to 14 GHz, and a 330-ps maximum time delay range was obtained. Such a time delay line is continuously variable and has the advantage of the operation at a fixed wavelength, which simplifies the architecture of beamforming systems in phased array microwave antennas. However, the economical and practical benefits of our approach cannot be assessed until systems tests are performed because of the additional electrical components which are required for each fiber grating.

References

[1] I. Frigies and A. J. Seeds, "Optically generated true-time delay in phased array antennas," *IEEE Trans. Microwave Theory Tech.*, vol. 43, pp. 2378–2386, 1995.

[2] D. T. K. Tong and M. C. Wu, "A novel multiwavelength optically controlled phased array antenna with a programmable dispersion matrix," *IEEE Photon. Technol. Lett.*, vol. 8, pp. 812–814, 1996.

[3] D. A. Cohen, Y. Chang, A. F. J. Levi, H. R. Fetterman, and I. L. Newberg, "Optically controlled serially fed phased array sensor," *IEEE Photon. Technol. Lett.*, vol. 8, pp. 1683–1685, 1996.

[4] G. A. Ball, W. H. Glenn, and W. W. Morey, "Programmable fiber optic delay line," *IEEE Photon. Technol. Lett.*, vol. 6, pp. 741–743, 1994.

[5] D. T. K. Tong and M. C. Wu, "Programmable dispersion matrix using fiber Bragg grating for optically controlled phase array antennas," *Electron. Lett.*, vol. 32, pp. 1532–1533, 1996.

[6] H. Zmuda, R. A. Soref, P. Payson, S. Jhons, and E. N. Toughlian, "Photonic beamformer for phased array antennas using a fiber grating prism," *IEEE Photon. Technol. Lett.*, vol. 9, pp. 241–243, 1997.

[7] A. Molony, C. Edge, and I. Bennion, "Fiber grating time delay for phased array antennas," *Electron. Lett.*, vol. 31, pp. 1485–1486, 1995.

[8] J. L. Cruz, B. Ortega, M. V. Andrés, B. Gimeno, D. Pastor, J. Capmany, and L. Dong, "Chirped fiber Bragg gratings for phased array antennas," *Electron. Lett.*, vol. 33, pp. 545–546, 1997.

[9] J. L. Cruz, B. Ortega, M. V. Andrés, B. Gimeno, J. Capmany, and L. Dong, "Array factor of a phased array antenna steered by a chirped fiber grating beamformer," *IEEE Photon. Technol. Lett.*, vol. 10, pp. 1153–1155, 1998.

[10] J. E. Román, M. Y. Frankel, P. J. Mattews, and R. D. Esman, "Time-steered array with a chirped grating beamformer," *Electron. Lett.*, vol. 33, pp. 652–653, 1997.
[11] B. Ortega, J. L. Cruz, J. Capmany, M. V. Andrés, and M. V. Pastor, "Variable delay line for phased array antenna based on a chirped fiber grating," *IEEE Trans. Microwave Theory Tech.*, vol. 47, pp. 1321–1326, July 1999.
[12] B. Ortega, J. L. Cruz, M. V. Andrés, A. Díez, D. Pastor, and J. Capmany, "A novel microwave phase shifted based on a fiber Bragg grating," *Electron. Lett.*, vol. 34, pp. 2051–2053, 1998.
[13] G. W. Yoffe, G. E. T. Arkwright, and B. G. Smith, "Tunable optical delay-line based on a fiber Bragg grating," *Electron. Lett.*, vol. 34, pp. 1688–1690-, 1998.
[14] J. L. Cruz, L. Dong, S. Barcelos, and L. Reekie, "Fiber Bragg gratings with various chirp profiles made in etched tapers," *Appl. Opt.*, vol. 35, pp. 6781–6787, 1996.
[15] J. L. Cruz, A. Diez, M. V. Andres, A. Segura, B. Ortega, and L. Dong, "Fiber Bragg gratings tuned and chirped using magnetic fields," *Electron. Lett.*, vol. 33, pp. 235–236, 1997.
[16] D. Pastor, B. Ortega, J. Capmany, J. L. Cruz, J. Martí, M. V. Andrés, E. Peral, M. J. Cole, and R. I. Laming, "Fully automatic simultaneous fiber grating amplitude and group delay characterization," *Microwave Optic. Technol. Lett.*, vol. 14, pp. 373–375, 1997.

Beatriz Ortega, photograph and biography not available at the time of publication.

José L. Cruz, photograph and biography not available at the time of publication.

José Capmany, photograph and biography not available at the time of publication.

Miguel V. Andrés, photograph and biography not available at the time of publication.

Daniel Pastor, photograph and biography not available at the time of publication.